

Dissociative recombination in krypton: Dependence of the total rate coefficient and excited-state production on electron temperature

Yueh-Jaw Shiu and Manfred A. Biondi

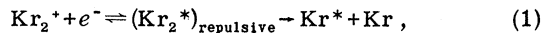
Department of Physics and Astronomy, University of Pittsburgh, Pittsburgh, Pennsylvania 15260

(Received 1 August 1977)

Microwave afterglow and grating spectrometric apparatus are used to study dissociative recombination in krypton. Over the electron temperature range $300 \leq T_e \leq 8400$ K and with $T_+ = T_{\text{gas}} = 300$ K, the total rate coefficient may be represented by $\alpha[\text{Kr}_2^+] = 1.6 \times 10^{-6} [300/T_e(\text{K})]^{0.55} \text{ cm}^3/\text{sec}$, with an uncertainty of $\pm 10\%$. At thermal energy (300 K) excited states of Kr^* having energies up to that of the Kr_2^+ ion in its ground electronic and vibrational state are observed to result from the dissociative recombination. With microwave heating to $T_e \sim 7000$ K, additional, higher-lying Kr^* states (up to ~ 0.5 eV above the Kr_2^+ ion ground state) are observed. In both cases the excited states most strongly populated by dissociative recombination appear to be the $5p$ states.

I. INTRODUCTION

The present study of the dissociative recombination of Kr_2^+ ions with electrons



is a continuation of our investigation of the properties of electron capture by the diatomic molecular ions of the heavier noble gases.¹ As such it is of interest not only for the insight it provides concerning the nature of the dissociative capture process but also for application to modelling of excimer lasers such as the KrF laser. Microwave afterglow techniques employing microwave heating of the electrons and high-speed spectrometric techniques are used¹ to determine the dependence on electron temperature of the total rate coefficient $\alpha(\text{Kr}_2^+)$ and the formation of specific excited states over the range $300 \leq T_e \leq 8400$ K. Previous studies of recombination in krypton^{2,3} have been carried out at room temperature under conditions such that $T_e = T_+ = T_n = 300$ K (the subscripts e , $+$, and n indicate electron, ion, and neutral gas, respectively).

II. MEASUREMENT TECHNIQUES

The microwave cavity-waveguide afterglow apparatus and grating spectrometer used in these studies has been described in detail previously.^{1,4} In the present studies a microwave discharge lasting ~ 1.5 msec and repeated at a 60-Hz rate is employed. The "microwave-averaged" electron density $\bar{n}_{\mu w}$ is determined during the afterglow from measurements of the resonant frequency shift of the high-Q TM_{010} cavity mode of the apparatus, while the electron temperature is controlled by steady microwave heating using the non-resonant TE_{11} circular waveguide mode of the apparatus. The spectrometric apparatus can detect

afterglow emission lying in the wavelength range $\sim 3000 < \lambda < 8900 \text{ \AA}$.

The krypton gas samples introduced via the ultrahigh-vacuum gas-handling system (base pressure $\sim 2 \times 10^{-9}$ Torr) are Union Carbide (Linde Div.) Research Grade gases and contain less than a few ppm of other gases, with the exception of xenon (~ 25 ppm). At the typical krypton pressures (~ 10 Torr) and microwave frequencies (~ 3 GHz) employed, the correction of the frequency-shift data for finite collision frequency effects is small ($\leq 4\%$) for the electron temperatures of interest.

As in previous studies the recombination coefficient α is determined by comparing the measured variation of $\bar{n}_{\mu w}$ during the afterglow with values obtained by computer solution of the electron continuity equation⁴

$$\frac{\partial n_e(\vec{r}, t)}{\partial t} \simeq -\alpha n_e^2 + D_a \nabla^2 n_e, \quad (2)$$

appropriate for a recombination-dominated afterglow with only one ion species of importance (here, Kr_2^+), so that $n_e \simeq n_+$. Known values of the ambipolar diffusion coefficient $D_a = D_+(1 + T_e/T_+)$, obtained from the measured mobility of Kr_2^+ in Kr,⁵ are used in Eq. (2) and $\alpha(\text{Kr}_2^+)$ is treated as a parameter to obtain the best fit to the measured electron density decays.

III. RESULTS

Examples of the measured electron decays at various electron temperatures are given in Fig. 1. The data are plotted in the form $1/\bar{n}_{\mu w}$ vs t , since in the limit of small diffusion loss the solution of Eq. (2) is $1/n_e(\vec{r}, t) = 1/n_e(\vec{r}, 0) + \alpha t$, the well-known "recombination decay." The solid lines through the data points are the computer solutions of Eq. (2). Deviations from the straight-line recombina-

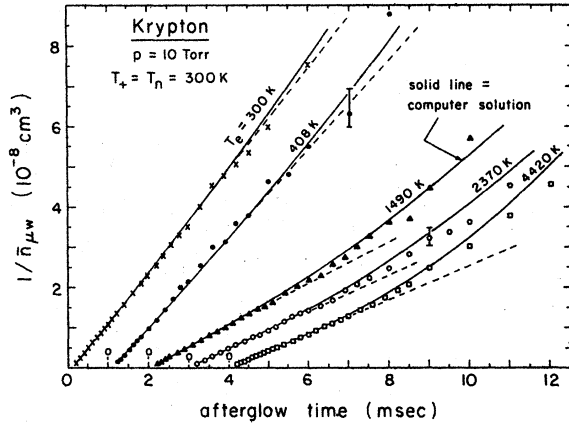


FIG. 1. Reciprocal of the "microwave averaged" electron density vs time, with electron temperature as a parameter. The zero afterglow times of successive curves are displaced 1 msec for clarity. The solid lines are fits to the data of computer solutions of Eq. (2). The error bar indicates the uncertainty in the $1/\bar{n}_{\mu w}$ values at low-electron densities.

tion-decay form, which result from the increasing importance of ambipolar diffusion loss in the late afterglow, are more apparent at the higher electron temperatures.

The inferred values of $\alpha(\text{Kr}_2^+)$ as a function of T_e are shown in Fig. 2. Although most of the measurements were carried out at $p(\text{Kr}) \approx 10$ Torr, no systematic variation of $\alpha(\text{Kr}_2^+)$ was found over the pressure range 5–15 Torr. Within the $\sim \pm 10\%$ uncertainty in the determinations the variation with electron temperature can be represented by

$$\alpha(\text{cm}^3/\text{sec}) = 1.6 \times 10^{-6} [300/T_e(\text{K})]^{0.55}. \quad (3)$$

The excited states formed by the dissociative

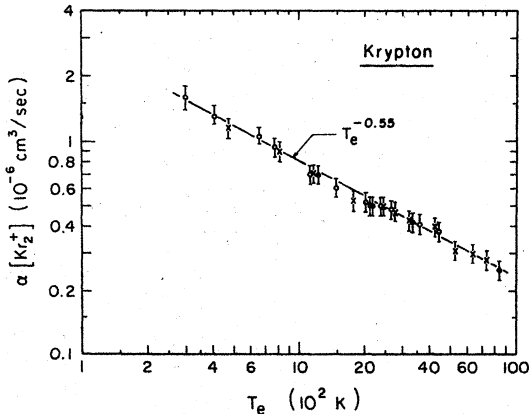


FIG. 2. Measured variation of $\alpha(\text{Kr}_2^+)$ with electron temperature for $T_e = T_n = 300$ K. The solid line represents a simple power-law variation as $T_e^{-0.55}$.

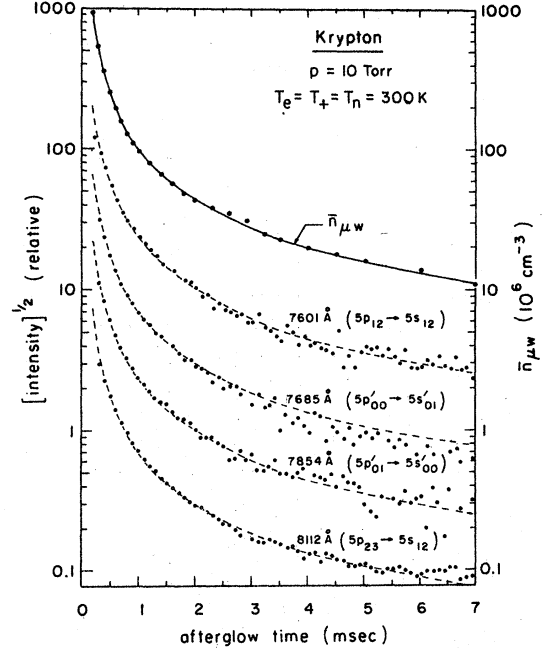


FIG. 3. Comparison of the variation of electron density $\bar{n}_{\mu w}$ and the square root of the afterglow intensity $I^{1/2}$ for representative transitions for the case $T_e = T_n = 300$ K. The dashed lines through the $I^{1/2}$ data represent renormalized $\bar{n}_{\mu w}$ data.

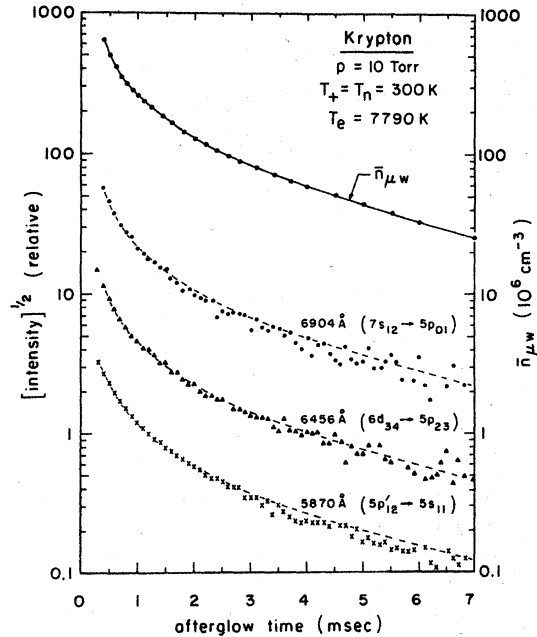


FIG. 4. Comparison of the variation of $\bar{n}_{\mu w}$ and $I^{1/2}$ during the afterglow for the case $T_e = 7790$ K, $T_n = 300$ K. Same format as Fig. 3.

TABLE I. Transitions originating from dissociative recombination of Kr_2^+ ions and electrons and their relative intensities in unheated ($T_e=300$ K) and heated ($T_e=6500$ K) afterglows. Modified Racah notation is used to designate the states.

Wavelength (Å)	Upper state	Lower state	Intensity	
			$T_e=300$ K	$T_e=6500$ K
4273	$6p_{12}$	$5s_{12}$	30	17
4282	$6p_{11}$	$5s_{12}$	2	1
4318	$6p_{22}$	$5s_{12}$	33	23
4319	$6p_{23}$	$5s_{12}$		
4362	$6p_{01}$	$5s_{12}$		
4376	$6p_{00}$	$5s_{11}$	4	4
4453	$6p_{12}$	$5s_{11}$	8	11
4463	$6p_{11}$	$5s_{11}$	5	6
4502	$6p_{22}$	$5s_{11}$	9	9
4562	$5p'_{12}$	$5s_{12}$	7	8
5562	$5p'_{12}$	$5s_{12}$	8	6
5570	$5p'_{01}$	$5s_{12}$	31	14
5580	$6p_{00}$	$5s'_{01}$	1	2
5649	$6p_{01}$	$5s'_{00}$	2	2
5866	$6p_{01}$	$5s'_{01}$	3	3
5870	$5p'_{12}$	$5s_{11}$	39	5
5879	$5p'_{01}$	$5s_{11}$	2	1
6056	$6d_{01}$	$5p_{01}$...	1
6421	$6d_{33}$	$5p_{22}$...	3
6456	$6d_{34}$	$5p_{23}$...	6
6904	$7s_{12}$	$5p_{01}$...	4
7224	$5d_{12}$	$5p_{01}$...	6
7287	$6s'_{01}$	$5p_{01}$...	4
7425	$7s_{11}$	$5p_{22}$...	2
7486	$6s'_{00}$	$5p_{01}$...	6
	$7s_{12}$	$5p_{23}$		
7587	$5p_{00}$	$5s_{11}$	290	62
7601	$5p_{12}$	$5s_{12}$	600	220
7685	$5p'_{00}$	$5s'_{01}$	190	110
7694	$5p_{11}$	$5s_{12}$	130	75
7746	$5d_{00}$	$5p_{01}$...	8
7854	$5p'_{01}$	$5s'_{00}$	270	150
7913	$5d_{01}$	$5p_{01}$	15	22
7928	$5d_{33}$	$5p_{22}$...	9
8059	$5p'_{11}$	$5s'_{00}$	160	120
8104	$5p_{22}$	$5s_{12}$	350	190
8112	$5p_{23}$	$5s_{12}$	1200	480
8190	$5p_{12}$	$5s_{11}$	480	250
8263	$5p'_{12}$	$4s'_{01}$	720	370
8281	$5p'_{01}$	$5s'_{01}$	170	170
8298	$5p_{11}$	$5s_{11}$	730	430
8509	$5p'_{11}$	$5s'_{01}$	130	190
8776	$5p_{22}$	$5s_{11}$	980	1100
8928	$5p_{01}$	$5s_{12}$	1000	1000

capture of electrons by Kr_2^+ ions are identified by the fact that, when such a two-body recombination process is the source of the excited states, the square root of the intensity of the resulting radiation follows the electron density variation during the afterglow. Examples of some typical transitions are shown for the unheated case, $T_e = T_n = 300$ K, in Fig. 3 and for a heated case, $T_e = 7790$ K,

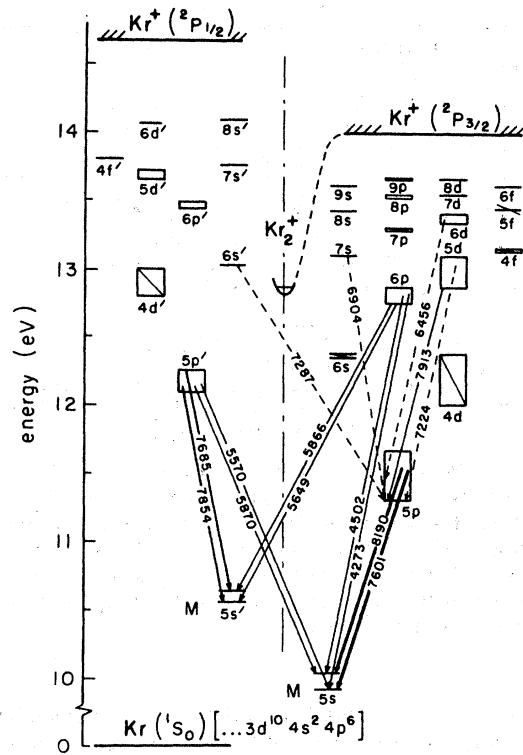


FIG. 5. Partial energy-level diagram for krypton showing representative transitions observed from dissociative recombination of Kr_2^+ ions and electrons. Modified Racah notation is used to designate the states. The weights of the lines indicate qualitatively the emission intensity; solid lines, $T_e = T_n = 300$ K; dashed lines $T_e = 6500$ K. A diagonal line through a state indicates that transitions from that state fall outside our wavelength-detection range.

in Fig. 4. Excellent tracking between \sqrt{I} and $\bar{n}_{\mu\nu}$ is observed.

A total of 31 transitions which exhibit a recombination origin were identified for the unheated ($T_e = 300$ K) case and are listed in Table I, together with their relative intensities. Additional transitions resulting from recombination into higher-lying states were observed during heating to $T_e = 6500$ K; these are also listed in Table I. The relative intensities are determined by gating the photon counting circuitry on during the intervals 0.05–10 msec and 0.15–10 msec during the afterglow in the unheated and heated cases, respectively. At long wavelengths (> 8200 Å) there is considerable uncertainty in the relative intensities because of the sharply falling photocathode sensitivity with increasing wavelength. The location of a representative group of these transitions on an energy level diagram for krypton is given in Fig. 5.

IV. DISCUSSION AND CONCLUSIONS

A. Total rate coefficient

The value $\alpha(\text{Kr}_2^+) = (1.6 \pm 0.2) \times 10^{-6} \text{ cm}^3/\text{sec}$ obtained in the present studies at $T_e = T_+ = T_n = 300 \text{ K}$ is in satisfactory agreement with the value $(1.2 \pm 0.2) \times 10^{-6} \text{ cm}^3/\text{sec}$ obtained by Oskam and Mittelstadt,³ if realistic assessments of the experimental uncertainties are used. The electron temperature dependence $\alpha(\text{Kr}_2^+) \sim T_e^{-0.55}$, measured over the range $300 \leq T_e \leq 8400 \text{ K}$, is very close to the $T_e^{-1/2}$ dependence predicted⁶ for simple diatomic ions involved in the direct capture process (depicted in reaction 1). As indicated in Table II the results for krypton fit the trend noted for the other noble gases of (a) increasing recombination coefficients with increasing atomic number at 300 K and (b) dependences on electron temperature compatible with the $T_e^{-1/2}$ prediction of the simple theory of the direct dissociative process.

B. Excited states produced by recombination

The excited states formed by the dissociative recombination process in krypton mirror the behavior noted in xenon¹; namely, for the unheated case, $T_e = 300 \text{ K}$, no states of Kr^* are produced which lie appreciably above the energy of the Kr_2^+ ion in its ground electronic and $v=0$ vibrational state (see Fig. 5, where the solid lines indicate the observed transitions at $T_e = 300 \text{ K}$). The observation of the formation of a $5d$ and several $6p$ excited states lying $\leq 0.1 \text{ eV}$ below the Kr_2^+ ($v=0$) initial state of the system indicates that even weakly repulsive states of (Kr_2^*) are formed with substantial probability.

With electron heating to $T_e \simeq 6500 \text{ K}$ (mean electron energy $\sim 0.7 \text{ eV}$) additional excited states, lying as much as $\sim 0.5 \text{ eV}$ above the Kr_2^+ ($v=0$) state, are observed. Thus, as in the case of xenon, our findings are consistent with a dissociative recombination process in which all energetically accessible states are formed, implying either the existence of suitable crossings between the potential curves of the initial $(\text{Kr}_2^+ + e)$ state and of the intermediate $(\text{Kr}_2^*)_{\text{repulsive}}$ states or of "curve hopping" from one repulsive state to another as the excited

TABLE II. Dissociative recombination coefficients at $T_e = T_+ = T_n = 300 \text{ K}$ and their dependence on T_e , expressed as T_e^{-x} .

Ion	α ($10^{-7} \text{ cm}^3/\text{sec}$)	x	Ref.
Ne_2^+	(1.7 ± 0.1)	0.43	a, b
Ar_2^+	(8.5 ± 0.8)	0.67	c
Kr_2^+	(16 ± 2)	0.55	Present work
Xe_2^+	(23 ± 2)	0.72	d

^aL. Frommhold, M. A. Biondi, and F. J. Mehr, Phys. Rev. 165, 44 (1968).

^bJ. Philbrick, F. J. Mehr, and M. A. Biondi, Phys. Rev. 181, 271 (1969).

^cF. J. Mehr and M. A. Biondi, Phys. Rev. 176, 322 (1968).

^dY. J. Shiu, M. A. Biondi, and D. P. Sipler, Phys. Rev. A 15, 494 (1977).

molecule dissociates to reach the different separated atom states. Again, as with xenon, Kr^* excited states belonging to both the $^2P_{3/2}$ and $^2P_{1/2}$ Kr^+ ion cores are formed, a finding consistent with the fact that the electronic wave function of the Kr_2^+ ion (initial state of the system) is an admixture of both $^2P_{3/2}$ and $^2P_{1/2}$, and so both types of excited states are accessible as final states.

We are at present unable to determine the partial recombination coefficients for formation of particular excited states, even though we have determined the intensities for some of the transitions from that state, since we do not know the branching ratios into transitions lying outside our wavelength detection range and therefore cannot evaluate the total rate of formation of the excited state. The relative intensities given in Table I do suggest that the $5p$ states are by far the most strongly populated by dissociative recombination in both the case of no electron heating and heating to $\sim 7000 \text{ K}$.

ACKNOWLEDGMENTS

The authors are indebted to D. P. Sipler for assistance in the design and testing of the electronic circuitry. This research was supported, in part, by the Advanced Research Projects Agency of the Department of Defense and was monitored by ONR under Contract No. N00014-76-C-0098.

¹Y. J. Shiu, M. A. Biondi, and D. P. Sipler, Phys. Rev. A 15, 494 (1977).

²J. M. Richardson, Phys. Rev. 88, 895 (1952).

³H. J. Oskam and V. R. Mittelstadt, Phys. Rev. 132, 1445 (1963).

⁴L. Frommhold, M. A. Biondi, and F. J. Mehr, Phys. Rev. 165, 44 (1968).

⁵See, for example, E. W. McDaniel and E. A. Mason, *The Mobility and Diffusion of Ions in Gases* (Wiley, New York, 1973).

⁶See, for example, J. N. Bardsley and M. A. Biondi, in *Advances in Atomic and Molecular Physics*, edited by D. R. Bates (Academic, New York, 1970), Vol. 6.